

Deflation with POD vectors for Porous Media Flow

Kees Vuik ¹, Gabriela B. Diaz Cortes ¹, Jan Dirk Jansen ².

¹EECMS

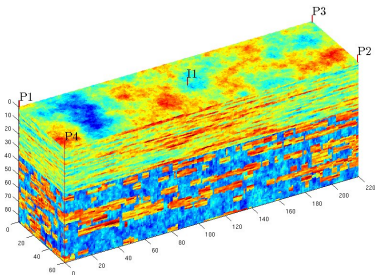
²CiTG

Delft University of Technology

The Seventh International Conference on Numerical Algebra and Scientific Computing (NASC 2019), October 19 till 23, 2019, Nanjing, P.R. China

SPE 10

Single-phase flow, grid size 60 x 220 x 85 grid cells.



| Method | Number of iterations |
|--------|----------------------|
| ICCG | 1011 |
| DICCG | 1 |

Table : Number of iterations for the SPE 10 benchmark (85 layers) for the ICCG and DICCG methods, tolerance of 10^{-7} .

Table of Contents

- 1 Problem Definition
- 2 DPCG
- 3 Deflation Vectors
- 4 Lemmas
- 5 Results
- 6 Conclusions
- 7 Bibliography

Reservoir Simulation

Single-phase flow through a porous media [1]

Darcy's law + mass balance equation

$$-\nabla \cdot \left[\frac{\alpha \rho}{\mu} \vec{\mathbf{K}} (\nabla \mathbf{p} - \rho g \nabla d) \right] + \alpha \rho \phi c_t \frac{\partial \mathbf{p}}{\partial t} - \alpha \rho \mathbf{q} = 0.$$

$$c_t = (c_l + c_r),$$

α a geometric factor

ρ fluid density

μ fluid viscosity

\mathbf{p} pressure

$\vec{\mathbf{K}}$ rock permeability

g gravity

d depth

ϕ rock porosity

\mathbf{q} sources

c_r rock compressibility

c_l liquid compressibility

Problem Definition

Discretization

3D case, isotropic permeability, small rock and fluid compressibilities, uniform reservoir thickness and no gravity forces.

$$-\frac{h}{\mu} \frac{\partial}{\partial x} \left(k \frac{\partial \mathbf{p}}{\partial x} \right) - \frac{h}{\mu} \frac{\partial}{\partial y} \left(k \frac{\partial \mathbf{p}}{\partial y} \right) - \frac{h}{\mu} \frac{\partial}{\partial z} \left(k \frac{\partial \mathbf{p}}{\partial z} \right) + h\phi_0 c_t \frac{\partial \mathbf{p}}{\partial t} - h\mathbf{q} = 0.$$

$$\mathcal{V} \dot{\mathbf{p}} + \mathcal{T} \mathbf{p} = \mathbf{q}.$$

\mathbf{q} : sources or wells in the reservoir, Peaceman well model, \mathcal{I}_{well} is the well index

$$\mathbf{q} = -\mathcal{I}_{well}(\mathbf{p} - \mathbf{p}_{well})$$

Accumulation matrix

$$\mathcal{V} = V c_t \phi_0 \mathcal{I},$$

$$V = h \Delta x \Delta y \Delta z.$$

Transmissibility matrix

$$\mathcal{T}_{i-\frac{1}{2},j,l} = \frac{\Delta y}{\Delta x \Delta z} \frac{h}{\mu} k_{i-\frac{1}{2},j,l},$$

$$k_{i-\frac{1}{2},j} = \frac{2}{\frac{1}{k_{i-1,j,l}} + \frac{1}{k_{i,j,l}}}.$$

Incompressible model

$$\mathcal{T}\mathbf{p} = \mathbf{q}.$$

Compressible model

$$\mathcal{V}^{n+1} \frac{(\mathbf{p}^{n+1} - \mathbf{p}^n)}{\Delta t^n} + \mathcal{T}^{n+1} \mathbf{p}^{n+1} = \mathbf{q}^{n+1}.$$

Or:

$$\mathcal{F}(\mathbf{p}^{n+1}; \mathbf{p}^n) = 0. \quad (1)$$

Using Newton-Raphson (NR) method, the system for the $(k + 1)$ -th NR iteration is:

$$\mathcal{J}(\mathbf{p}^k)\delta\mathbf{p}^{k+1} = -\mathcal{F}(\mathbf{p}^k; \mathbf{p}^n), \quad \mathbf{p}^{k+1} = \mathbf{p}^k + \delta\mathbf{p}^{k+1},$$

where $\mathcal{J}(\mathbf{p}^k) = \frac{\partial\mathcal{F}(\mathbf{p}^k; \mathbf{p}^n)}{\partial\mathbf{p}^k}$ is the Jacobian matrix, and $\delta\mathbf{p}^{k+1}$ is the NR update at iteration step $k + 1$.

$$\mathcal{J}(\mathbf{p}^k)\delta\mathbf{p}^{k+1} = \mathbf{b}(\mathbf{p}^k). \quad (2)$$

Conjugate Gradient Method (CG)

Successive approximations to obtain a more accurate solution \mathbf{x} [2]

$$\mathcal{A}\mathbf{x} = \mathbf{b},$$

$$\mathbf{x}^0, \quad \text{initial guess} \quad \mathbf{r}^{k-1} = \mathbf{b} - \mathcal{A}\mathbf{x}^{k-1}.$$
$$\min_{\mathbf{x}^k \in \kappa_k(\mathcal{A}, \mathbf{r}^0)} \|\mathbf{x} - \mathbf{x}^k\|_{\mathcal{A}}, \quad \|\mathbf{x}\|_{\mathcal{A}} = \sqrt{\mathbf{x}^T \mathcal{A} \mathbf{x}}.$$

Convergence

$$\|\mathbf{x} - \mathbf{x}^k\|_{\mathcal{A}} \leq 2\|\mathbf{x} - \mathbf{x}^0\|_{\mathcal{A}} \left(\frac{\sqrt{\kappa(\mathcal{A})} - 1}{\sqrt{\kappa(\mathcal{A})} + 1} \right)^k.$$

Preconditioning

Improve the spectrum of \mathcal{A} .

$$\mathcal{M}^{-1}\mathcal{A}\mathbf{x} = \mathcal{M}^{-1}\mathbf{b}.$$

Convergence

$$\|\mathbf{x} - \mathbf{x}^k\|_{\mathcal{A}} \leq 2\|\mathbf{x} - \mathbf{x}^0\|_{\mathcal{A}} \left(\frac{\sqrt{\kappa(\mathcal{M}^{-1}\mathcal{A})} - 1}{\sqrt{\kappa(\mathcal{M}^{-1}\mathcal{A})} + 1} \right)^k, \quad \kappa(\mathcal{M}^{-1}\mathcal{A}) \leq \kappa(\mathcal{A}).$$

DPCG history

- 1987 Nicolaides and Dostal
First versions of DPCG
- 1999 Vuik, Meijerink, Segal
DPCG applied to reservoir simulations (Shell)
- 2004 Nabben, Vuik
Theory and porous media flow
- 2008 Nabben, Tang, Vuik, ...
Theory comparison: DPCG, MG and Domain Decomposition, bubbly flow

DPCG history

- 2008 Nabben Erlangga
Convection diffusion, Helmholtz, MLK method
- 2010 Jönsthövel, Vuik
Mechanical problems, parallel computing
- 2014 Nabben, Sheikh, Lahaye, Vuik, Garcia
MLK/ADEF method Helmholtz equation
- 2016 Diaz, Jansen, Vuik
Porous media flow, Model Order Reduction (MOR)

Deflation

$$\begin{aligned}
 \mathcal{P} &= \mathcal{I} - \mathcal{A}\mathcal{Q}, & \mathcal{P} &\in \mathbb{R}^{n \times n}, & \mathcal{Q} &\in \mathbb{R}^{n \times n}, \\
 \mathcal{Q} &= \mathcal{Z}\mathcal{E}^{-1}\mathcal{Z}^T, & \mathcal{Z} &\in \mathbb{R}^{n \times k}, & \mathcal{E} &\in \mathbb{R}^{k \times k}, \\
 & & \mathcal{E} &= \mathcal{Z}^T \mathcal{A} \mathcal{Z} \text{ (Tang 2008, [3])}.
 \end{aligned}$$

Convergence

Deflated system

$$\|\mathbf{x} - \mathbf{x}^k\|_{\mathcal{A}} \leq 2\|\mathbf{x} - \mathbf{x}^0\|_{\mathcal{A}} \left(\frac{\sqrt{\kappa_{\text{eff}}(\mathcal{P}\mathcal{A})} - 1}{\sqrt{\kappa_{\text{eff}}(\mathcal{P}\mathcal{A})} + 1} \right)^k.$$

Deflated and preconditioned system

$$\|\mathbf{x} - \mathbf{x}^k\|_{\mathcal{A}} \leq 2\|\mathbf{x} - \mathbf{x}^0\|_{\mathcal{A}} \left(\frac{\sqrt{\kappa_{\text{eff}}(\mathcal{M}^{-1}\mathcal{P}\mathcal{A})} - 1}{\sqrt{\kappa_{\text{eff}}(\mathcal{M}^{-1}\mathcal{P}\mathcal{A})} + 1} \right)^k.$$

$$\kappa_{\text{eff}}(\mathcal{M}^{-1}\mathcal{P}\mathcal{A}) \leq \kappa_{\text{eff}}(\mathcal{P}\mathcal{A}) \leq \kappa(\mathcal{A}).$$

Recycling deflation (Clemens 2004, [4]).

$$\mathcal{Z} = [\mathbf{x}^1, \mathbf{x}^2, \mathbf{x}^{q-1}],$$

\mathbf{x}^i 's are solutions of the system.

Multigrid and multilevel (Tang 2009, [5]).

The matrices \mathcal{Z} and \mathcal{Z}^T are the restriction and prolongation matrices of multigrid methods.

Subdomain deflation (Vuik 1999,[6]).

Model Order Reduction (MOR)

Many modern mathematical models of real-life processes pose challenges when used in numerical simulations, due to complexity and large size.

Model order reduction aims to lower the computational complexity of such problems by a reduction of the model's associated state space dimension or degrees of freedom, an approximation to the original model is computed. (Vuik 2005, [7])

- Proper Orthogonal Decomposition (POD)
- Reduced Basis Method (RBM)
- Principal Component Analysis (PCA)
- Singular Value Decomposition (SVD)

Proposal

Use solution of the system with diverse well configurations '*snapshots*' as deflation vectors (Recycling deflation).

Use as deflation vectors the basis obtained from Proper Orthogonal Decomposition (POD).

Proper Orthogonal Decomposition (POD)

POD: find an 'optimal' basis for a given data set (Markovinović 2009 [8], Astrid 2011, [9])

- Get the snapshots

$$\mathcal{X} = [\mathbf{x}_1, \mathbf{x}_2, \dots, \mathbf{x}_m].$$

- Form \mathcal{R}

$$\mathcal{R} := \frac{1}{m} \mathcal{X} \mathcal{X}^T \equiv \frac{1}{m} \sum_{i=1}^m \mathbf{x}_i \mathbf{x}_i^T.$$

- Then

$$\Phi = [\phi_1, \phi_2, \dots, \phi_l] \in \mathbb{R}^{n \times l}$$

are the l eigenvectors corresponding to the largest eigenvalues of \mathcal{R} satisfying:

$$\frac{\sum_{j=1}^l \lambda_j}{\sum_{j=1}^m \lambda_j} \leq \alpha, \quad 0 < \alpha \leq 1.$$

Lemma 1

Let $\mathcal{A} \in \mathbb{R}^{n \times n}$ be a non-singular matrix, and \mathbf{x} is a solution of:

$$\mathcal{A}\mathbf{x} = \mathbf{b}. \quad (3)$$

Let $\mathbf{x}_i, \mathbf{b}_i \in \mathbb{R}^n$, $i = 1, \dots, m$, be vectors linearly independent (*l.i.*) and

$$\mathcal{A}\mathbf{x}_i = \mathbf{b}_i. \quad (4)$$

The following equivalence holds

$$\mathbf{x} = \sum_{i=1}^m c_i \mathbf{x}_i \quad \Leftrightarrow \quad \mathbf{b} = \sum_{i=1}^m c_i \mathbf{b}_i. \quad (5)$$

Lemma 1 (proof)

$$\text{Proof} \Rightarrow \quad \mathbf{x} = \sum_{i=1}^m c_i \mathbf{x}_i \Rightarrow \mathbf{b} = \sum_{i=1}^m c_i \mathbf{b}_i. \quad (6)$$

Substituting \mathbf{x} from (6) into $\mathcal{A}\mathbf{x} = \mathbf{b}$ and using the linearity of \mathcal{A} we obtain:

$$\mathcal{A}\mathbf{x} = \sum_{i=1}^m c_i \mathcal{A}\mathbf{x}_i = \sum_{i=1}^m c_i \mathbf{b}_i = \mathbf{b}. \quad \text{Similarly for } \Leftarrow \quad \boxtimes$$

Lemma 2

If the deflation matrix \mathcal{Z} is constructed with a set of m vectors

$$\mathcal{Z} = [\mathbf{x}_1 \quad \dots \quad \dots \quad \mathbf{x}_m], \quad (7)$$

such that $\mathbf{x} = \sum_{i=1}^m c_i \mathbf{x}_i$, with \mathbf{x}_i *l.i.*, then the solution of system (3) is obtained with one iteration of DCG.

Lemma 2 (proof)

Proof.

The relation between $\hat{\mathbf{x}}$ and \mathbf{x} is given by [3]:

$$\mathbf{x} = \mathcal{Q}\mathbf{b} + \mathcal{P}^T \hat{\mathbf{x}}.$$

For the first term $\mathcal{Q}\mathbf{b}$, taking $\mathbf{b} = \sum_{i=1}^m c_i \mathbf{b}_i$ we have:

$$\begin{aligned} \mathcal{Q}\mathbf{b} &= \mathcal{Z}\mathcal{E}^{-1}\mathcal{Z}^T \left(\sum_{i=1}^m c_i \mathbf{b}_i \right) = \mathcal{Z}(\mathcal{Z}^T \mathcal{A}\mathcal{Z})^{-1} \mathcal{Z}^T \left(\sum_{i=1}^m c_i \mathcal{A}\mathbf{x}_i \right) \\ &= \mathcal{Z}(\mathcal{Z}^T \mathcal{A}\mathcal{Z})^{-1} \mathcal{Z}^T (\mathcal{A}\mathbf{x}_1 c_1 + \dots + \mathcal{A}\mathbf{x}_m c_m) = \mathcal{Z}(\mathcal{Z}^T \mathcal{A}\mathcal{Z})^{-1} (\mathcal{Z}^T \mathcal{A}\mathcal{Z})\mathbf{c} \\ &= \mathcal{Z}\mathbf{c} = c_1 \mathbf{x}_1 + c_2 \mathbf{x}_2 + \dots + c_m \mathbf{x}_m = \sum_{i=1}^m c_i \mathbf{x}_i = \mathbf{x}. \end{aligned}$$

Lemma 2 (proof)

Therefore,

$$\mathbf{x} = \mathcal{Q}\mathbf{b}, \quad (8)$$

is the solution to the original system.

For the second term of the equation, $\mathcal{P}^T \hat{\mathbf{x}}$, we compute the deflated solution $\hat{\mathbf{x}}$.

$$\mathcal{P}\mathcal{A}\hat{\mathbf{x}} = \mathcal{P}\mathbf{b}$$

$$\mathcal{A}\mathcal{P}^T \hat{\mathbf{x}} = (\mathcal{I} - \mathcal{A}\mathcal{Q})\mathbf{b} \quad \text{using } \mathcal{A}\mathcal{P}^T = \mathcal{P}\mathcal{A} \text{ [3] and definition of } \mathcal{P},$$

$$\mathcal{A}\mathcal{P}^T \hat{\mathbf{x}} = \mathbf{b} - \mathcal{A}\mathcal{Q}\mathbf{b}$$

$$\mathcal{A}\mathcal{P}^T \hat{\mathbf{x}} = \mathbf{b} - \mathcal{A}\mathbf{x} = 0$$

taking $\mathcal{Q}\mathbf{b} = \mathbf{x}$ from above,

$$\mathcal{P}^T \hat{\mathbf{x}} = 0$$

as \mathcal{A} is invertible.

Then we have obtained the solution

$$\mathbf{x} = \mathcal{Q}\mathbf{b} + \mathcal{P}^T \hat{\mathbf{x}} = \mathcal{Q}\mathbf{b},$$

in one step of DCG.

Single-phase, $\mathbf{T}\mathbf{p}^n = \mathbf{q}^n$

Recycling linearly independent (l.i.) solutions

Compute l.i.
solutions with ICCG

$$\mathbf{T}\mathbf{p}_i = \mathbf{q}_i,$$

Construct \mathbf{Z}

$$\mathbf{Z} = \begin{bmatrix} \mathbf{p}_1 & \cdots & \mathbf{p}_n \end{bmatrix},$$

Use \mathbf{Z} to solve
with DICCG

$$\mathbf{T}\mathbf{p} = \mathbf{q}.$$

Two-phases, $\mathbf{T}^n \mathbf{p}^n = \mathbf{q}^n$

Training phase approach

Compute snapshots
with ICCG

Construct
correlation matrix

Obtain POD basis
and use it
to construct \mathbf{Z}_m

$$\mathbf{T}^i \mathbf{p}^i = \mathbf{q}^i,$$

$$\mathbf{C} = \mathbf{X}\mathbf{X}^T$$

$$\mathbf{Z} = [\phi_1, \dots, \phi_n]$$

$$\mathbf{X} = [\mathbf{p}^1 \dots \mathbf{p}^n]$$

Use \mathbf{Z} to solve $\mathbf{T}\mathbf{p} = \mathbf{q}$ with DICCG, different problems.

Numerical experiments

Heterogeneous permeability (Neumann and Dirichlet boundary conditions).

The experiments were performed for single-phase flow, with the following characteristics:

$n_x = n_y = 64$ grid cells.

5 linearly independent snapshots.

| System configuration | | | | | | | | |
|-----------------------|----|----|----|----------------------------|----------|------------|--------------------------------------|--|
| Well pressures (bars) | | | | Boundary conditions (bars) | | | | |
| | W1 | W2 | W3 | W4 | $P(y=0)$ | $P(y=L_y)$ | $\frac{\partial P(x=0)}{\partial n}$ | $\frac{\partial P(x=L_x)}{\partial n}$ |
| | -5 | -5 | +5 | +5 | 0 | 3 | 0 | 0 |
| Snapshots | | | | | | | | |
| | W1 | W2 | W3 | W4 | $P(y=0)$ | $P(y=L_y)$ | $\frac{\partial P(x=0)}{\partial n}$ | $\frac{\partial P(x=L_x)}{\partial n}$ |
| z_1 | -5 | 0 | 0 | 0 | 0 | 0 | 0 | 0 |
| z_2 | 0 | -5 | 0 | 0 | 0 | 0 | 0 | 0 |
| z_3 | 0 | 0 | -5 | 0 | 0 | 0 | 0 | 0 |
| z_4 | 0 | 0 | 0 | -5 | 0 | 0 | 0 | 0 |
| z_5 | 0 | 0 | 0 | 0 | 0 | 3 | 0 | 0 |

Table : Table with the well configuration and boundary conditions of the system and the snapshots used for the Case 1.

Numerical experiments

Heterogeneous permeability (Neumann and Dirichlet boundary conditions).

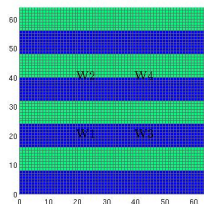


Figure : Heterogeneous permeability, 4 wells.

| κ_2 (mD) | 10^{-1} | 10^{-2} | 10^{-3} |
|-----------------|-----------|-----------|-----------|
| ICCG | 75 | 103 | 110 |
| DICCG | 1 | 1 | 1 |

Table : Number of iterations for different contrasts between the permeability of the layers for the ICCG and DICCG methods.

Numerical experiments

Heterogeneous permeability (Neumann boundary conditions).

The experiments were performed for single-phase flow, with the following characteristics:

$n_x = n_y = 64$ grid cells.

Neumann boundary conditions.

15 snapshots, 4 linearly independent.

$W_1 = W_2 = W_3 = W_4 = -1$ bars,

$W_5 = +4$ bars.

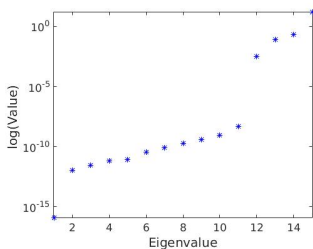


Figure : Eigenvalues of the data snapshot correlation matrix.

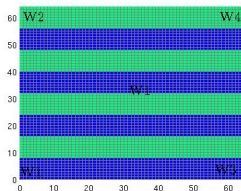


Figure : Heterogeneous permeability layers.

| σ_2 (mD) | 10^{-1} | 10^{-2} | 10^{-3} |
|----------------------------------|-----------|-----------|-----------|
| ICCG | 90 | 115 | 131 |
| DICCG ₄ | 1 | 1 | 1 |
| DICCG ₁₅ | 200* | 200* | 200* |
| DICCG _{POD₄} | 1 | 1 | 1 |

Table : Number of iterations.

Numerical experiments

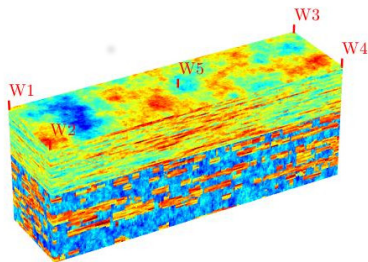
SPE 10 model

60x220x85 grid cells.

Neumann boundary conditions.

15 snapshots, 4 linearly independent.

$W1 = W2 = W3 = W4 = -1$ bars, $W5 = +4$ bars.



| Method | Iterations |
|-----------------------|------------|
| ICCG | 1011 |
| DICCG ₁₅ | 2000* |
| DICCG ₄ | 1 |
| DICCG _{POD4} | 1 |

Table : Number of iterations for ICCG and DICCG methods.

Figure : SPE 10 benchmark, permeability field.

Numerical experiments

Compressible heterogeneous layered problem

35x35 grid cells.

Neumann boundary conditions.

$W1 = W2 = W3 = W4 = 100$ bars, $W5 = 600$ bars.

Initial pressure 200 bars.

Contrast between permeability layers of 10^1 , 10^2 and 10^3 .

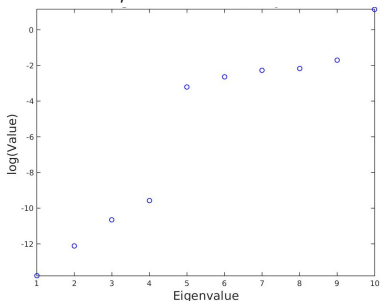
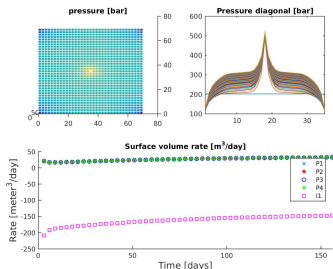


Figure : Solution, contrast between permeability layers of 10^1 .

Figure : Eigenvalues of the data snapshot correlation matrix, contrast between permeability layers of 10^1 .

Numerical experiments

| 1 st NR Iteration | | | | | | |
|------------------------------|---------------------|----------------------------------|-------------------|-------|---------------------|--------------------------|
| $\frac{\sigma_2}{\sigma_1}$ | Total ICCG(only) | Method | ICCG Snapshots | DICCG | Total ICCG+DICCG | % of total ICCG(only) |
| 10^1 | 780 | DICCG ₁₀ | 140 | 42 | 182 | 23 |
| | 780 | DICCG _{POD₆} | 140 | 84 | 224 | 29 |
| 10^2 | 624 | DICCG ₁₀ | 100 | 42 | 142 | 23 |
| | 624 | DICCG _{POD₇} | 100 | 42 | 142 | 23 |
| 10^3 | 364 | DICCG ₁₀ | 20 | 42 | 62 | 17 |
| | 364 | DICCG _{POD₇} | 20 | 42 | 62 | 17 |

Table : Comparison between the ICCG and DICCG methods of the average number of linear iterations for the first NR iteration for various contrast between permeability layers.

| 2 nd NR Iteration | | | | | | |
|------------------------------|---------------------|----------------------------------|-------------------|-------|---------------------|--------------------------|
| $\frac{\sigma_2}{\sigma_1}$ | Total ICCG(only) | Method | ICCG Snapshots | DICCG | Total ICCG+DICCG | % of total ICCG(only) |
| 10^1 | 988 | DICCG ₁₀ | 180 | 78 | 258 | 26 |
| | 988 | DICCG _{POD₆} | 180 | 198 | 378 | 38 |
| 10^2 | 832 | DICCG ₁₀ | 140 | 90 | 230 | 28 |
| | 832 | DICCG _{POD₇} | 140 | 154 | 294 | 33 |
| 10^3 | 884 | DICCG ₁₀ | 110 | 90 | 200 | 23 |
| | 884 | DICCG _{POD₇} | 110 | 150 | 260 | 29 |

Table : Comparison between the ICCG and DICCG methods of the average number of linear iterations for the second NR iteration for various contrast between permeability layers.

Numerical experiments

Compressible SPE 10 problem

60x220x85 grid cells.

Neumann boundary conditions.

$W1 = W2 = W3 = W4 = 100$ bars, $W5 = 600$ bars.

Initial pressure 200 bars.

Contrast in permeability of 3×10^7 .

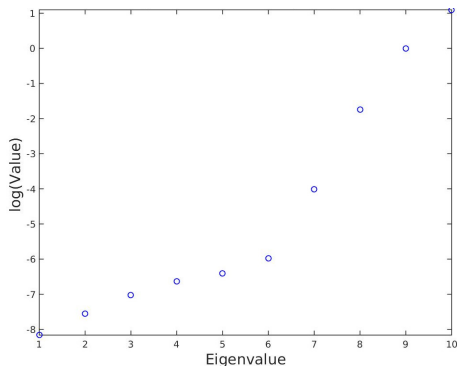


Figure : Eigenvalues of the data snapshot correlation matrix.

Numerical experiments

| 1 st NR Iteration | | | | | |
|------------------------------|----------------------------------|----------------|-------|------------------|-----------------------|
| Total ICGG(only) | Method | ICCG Snapshots | DICCG | Total ICGG+DICCG | % of total ICGG(only) |
| 10173 | DICCG ₁₀ | 1770 | 1134 | 2904 | 28 |
| 10173 | DICCG _{POD₄} | 1770 | 1554 | 3324 | 32 |

Table : Total number of linear iterations for the first NR iteration, full SPE 10 benchmark.

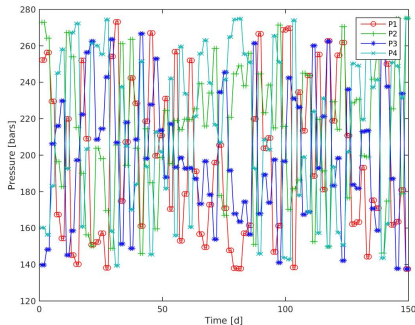
| 2 nd NR Iteration | | | | | |
|------------------------------|----------------------------------|----------------|-------|------------------|-----------------------|
| Total ICGG(only) | Method | ICCG Snapshots | DICCG | Total ICGG+DICCG | % of total ICGG(only) |
| 10231 | DICCG ₁₀ | 1830 | 200 | 2030 | 20 |
| 10231 | DICCG _{POD₄} | 1830 | 200 | 2030 | 20 |

Table : Total number of linear iterations for the second NR iteration, full SPE 10 benchmark.

Numerical experiments, two-phase flow

Injection through wells, *training phase approach*

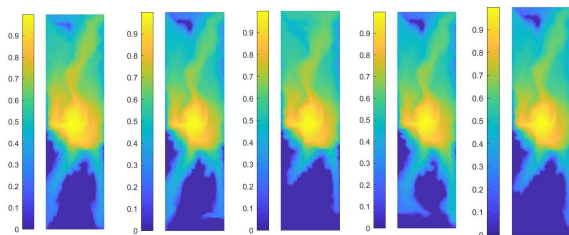
| Well pressures [bars], $P_0 = 500$ [bars] | | | | |
|---|---------|---------|---------|------|
| Training phase | | | | |
| $P1$ | $P2$ | $P3$ | $P4$ | I |
| 137-275 | 137-275 | 137-275 | 137-275 | 1100 |
| Same pressure in the producers | | | | |
| 200 | 200 | 200 | 200 | 800 |
| Different pressure in the producers | | | | |
| 20 | 500 | 500 | 500 | 4xP |



Numerical experiments, two-phase flow

Injection through wells, *training phase approach*

Pressure Field



Same pressure in production wells
 $P_{bhp} = 200$ [bars]

Different pressure in production wells
 $P_{2,3,4} = 500$ [bars], $P_1 = 20$ [bars]

| | Total | DICCG | % of ICGG |
|----|-------|--------|-----------|
| dv | ICGG | Method | |
| 10 | 90130 | 13720 | 15 |
| 5 | 90130 | 21522 | 24 |

| | Total | DICCG | % of ICGG |
|----|-------|--------|-----------|
| dv | ICGG | Method | |
| 10 | 90130 | 11740 | 13 |
| 5 | 90130 | 17855 | 20 |

Table : Number of iterations.

Numerical experiments, two-phase flow

Injection through wells, training phase approach

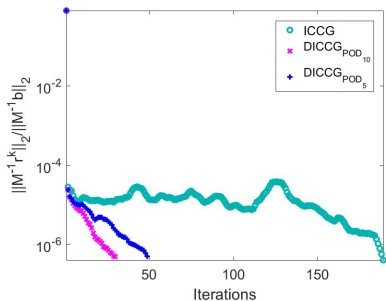


Figure : Relative residual.

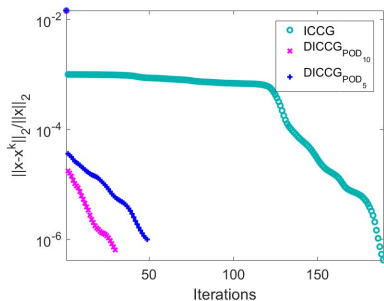


Figure : Relative true error.

- Solution is reached in few (1 or 2) iterations for the DICCG method in the incompressible case.
- A good choice of snapshots takes into account the boundary conditions of the problem.
- The number of iterations of the DICCG method does not depend on the contrast between the coefficients (Heterogeneous permeability example).
- The number of iterations of the ICCG method is reduced up to 80% with the DICCG method in the compressible case.
- Only a limited number of POD basis vectors is necessary to obtain a good speed-up. (for more info see [10, 11])

References I



J.D. Jansen.

A systems description of flow through porous media.
Springer, 2013.



Y. Saad.

Iterative Methods for Sparse Linear Systems.
Society for Industrial and Applied Mathematics Philadelphia, PA, USA. Society for Industrial and Applied Mathematics, 2nd edition, 2003.



J. Tang.

Two-Level Preconditioned Conjugate Gradient Methods with Applications to Bubbly Flow Problems.
PhD thesis, Delft University of Technology, 2008.



M. Clemens; M. Wilke; R. Schuhmann ; T. Weiland.

Subspace projection extrapolation scheme for transient field simulations.
IEEE Transactions on Magnetics, 40(2):934–937, 2004.



Jok Man Tang, Reinhard Nabben, Cornelis Vuik, and Yogi A Erlangga.

Comparison of two-level preconditioners derived from deflation, domain decomposition and multigrid methods.
Journal of scientific computing, 39(3):340–370, 2009.



C. Vuik; A. Segal; and J. A. Meijerink.

An Efficient Preconditioned CG Method for the Solution of a Class of Layered Problems with Extreme Contrasts in the Coefficients.
Journal of Computational Physics, 152:385–403, 1999.



C. Vuik.

Deflation acceleration for CFD problems.

Linear algebra and model order reduction, Model order reduction, coupled problems and optimization from 19 Sep 2005 through 23 Sep 2005, 1:1–1, 2005.



R. Markovinović.

System-Theoretical Model Reduction for Reservoir Simulation and Optimization.

PhD thesis, Delft University of Technology, 2009.



P. Astrid; G. Papaioannou; J. C Vink; J.D. Jansen.

Pressure Preconditioning Using Proper Orthogonal Decomposition.

In *2011 SPE Reservoir Simulation Symposium, The Woodlands, Texas, USA*, pages 21–23, January 2011.



G. B. Diaz Cortes, C. Vuik, and J. D. Jansen.

On POD-based deflation vectors for DPCG applied to porous media problems.

Journal of Computational and Applied Mathematics, 330:193–213, 2018.



G.B. Diaz Cortes, C. Vuik, and J.D. Jansen.

Physics-based pre-conditioners for large-scale subsurface flow simulation.

In J.D. Jansen, editor, *ECMOR XV - 15th European Conference on the Mathematics of Oil Recovery, August 29 - September 1, 2016*, pages 1–10, Houten, 2016. EAGE.

DOI: 10.3997/2214-4609.201601801.